BMP signaling is required to form the anterior neural plate border in ascidian embryos

Boqi Liu*, Ximan Ren, and Yutaka Satou

Department of Zoology, Graduate School of Science, Kyoto University,

Sakyo, Kyoto 606-8502, Japan

The first two authors contributed equally to this work.

Correspondence to yutaka@ascidian.zool.kyoto-u.ac.jp (Yutaka Satou)

ORCID: 0000-0002-4422-8766 (B.L.), 0000-0001-8955-1105 (X.R.), 0000-0001-5193-0708 (Y.S.)

*current address: State Key Laboratory of Biomembrane and Membrane Biotechnology, Tsinghua University–Peking University Joint Center for Life Sciences, School of Life Sciences, Tsinghua University, Beijing, China

Abstract

Cranial neurogenic placodes have been considered vertebrate innovations. However, anterior neural plate border (ANB) cells of ascidian embryos share many properties with vertebrate neurogenic placodes; therefore, it is now believed that the last common ancestor of vertebrates and ascidians had embryonic structures similar to neurogenic placodes of vertebrate embryos. Because BMP signaling is important for specifying the placode region in vertebrate embryos, we examined whether BMP signaling is also involved in gene expression in the ANB region of ascidian embryos. Our data indicated that Admp, a divergent BMP family member, is mainly responsible for BMP signaling in the ANB region, and that two BMP-antagonists, Noggin and Chordin, restrict the domain, in which BMP signaling is activated, in the ANB region, but not in the neural plate. BMP signaling is required for expression of *Foxg* and *Six1/2* at the late gastrula stage, and also for expression of *Zf220*, which encodes a zinc finger transcription factor in late neurula embryos. Because *Zf220* negatively regulates *Foxg*, when we downregulated *Zf220* by inhibiting BMP signaling, *Foxg* was upregulated, resulting in one large palp instead of three palps (adhesive organs derived from ANB cells). Functions of BMP signaling in specification of the ANB region give further support to the hypothesis that ascidian ANB cells share an evolutionary origin with vertebrate cranial placodes.

Keywords: ascidian, *Ciona*, placode, anterior neural plate border

Introduction

Cranial neurogenic placodes in vertebrate embryos are ectodermal thickenings at the anterior border of the neural plate. These placodes give rise to cells in various organs in the vertebrate head, including the adenohypophysis, olfactory epithelium, lens, inner ear, and petrosal and nodose ganglia (Schlosser, 2014; Singh and Groves, 2016; Steventon et al., 2014). It has been proposed that acquisition of these placodes remodeled rostral structures in the vertebrate lineage (Gans and Northcutt, 1983).

Ascidians belong to the sister group of vertebrates (Delsuc et al., 2006; Putnam et al., 2008), and previous studies have shown that the anterior neural plate border (ANB) region of ascidian embryos shares an evolutionary origin with vertebrate placodes (Abitua et al., 2015; Cao et al., 2019; Horie et al., 2018; Ikeda et al., 2013; Liu and Satou, 2019, 2020; Manni et al., 2005; Manni et al., 2004; Mazet et al., 2005). At the gastrula stage, two rows of ANB cells (four cells in each row), which express *Foxc*, are formed between the neural plate and non-neural ectoderm (Ikeda et al., 2013; Wagner and Levine, 2012) (Figure 1A). At the neurula stage, ANB cells divide once to yield four rows, each of which contains four cells. Cells in the most posterior row express transcription factor genes, *Six1/2* and *Foxg* (Abitua et al., 2015; Liu and Satou, 2019). The most anterior row also expresses *Foxg*, but not *Six1/2*. The second and third rows express *Emx*, which is repressed by *Foxg* in the most anterior and posterior rows (Liu and Satou, 2019; Wagner et al., 2014). The MAPK pathway is specifically activated in the most anterior and posterior rows, because it is negatively regulated by Ephrina.d in the middle two rows. This MAPK pathway specifically activates *Foxg* in the first and fourth rows. After the next division, the first and second anterior rows both include eight cells, and *Zf220* begins to be expressed in four cells in each row. *Foxg* expression becomes rarely visible, but soon after it is reactivated in descendant cells of the most anterior row. Because *Zf220* negatively regulates *Foxg*, *Foxg* expression becomes restricted in four cells, which do not express *Zf220*, in the first row at the middle tailbud stage (Liu and Satou, 2019). Thus, several distinct cell populations are specified in the ANB region. Among them, *Foxg*(+)/*Six1/2*(-) cells gives rise to the protrusive parts of the palps, which are adhesive organs required for metamorphosis. *Foxg*(-) cells contribute to basal parts of the palps.

Foxg(+)/*Six1/2*(+) cells give rise to the oral siphon primordium (Abitua et al., 2015; Liu and Satou, 2019; Wagner et al., 2014).

A previous study showed that misexpression of *Bmp2/4* or a constitutively active form of a BMP receptor in ANB cells downregulates expression of *Six1/2* (Abitua et al., 2015). Therefore, BMP signaling may be involved in formation and pattering of the ANB region of ascidian embryos as in formation of the pre-placodal region of vertebrate embryos, in which BMP signaling is essential to form placodes (Ahrens and Schlosser, 2005; Brugmann et al., 2004; Esterberg and Fritz, 2009; Glavic et al., 2004; Kwon et al., 2010; Litsiou et al., 2005). In the present study, we examined how BMP signaling contributes to patterning of ANB cells in ascidian embryos to explore developmental mechanisms of the last common ancestor of vertebrates and ascidians.

Materials and Methods

Animals and gene identifiers

Adult *Ciona robusta* (also called *Ciona intestinalis* type A) were obtained from the National Bio-Resource Project for *Ciona intestinalis*. This animal is excluded from legislation regulating scientific research on animals in Japan. cDNA clones were obtained from our EST clone collection (Satou et al., 2005). Identifiers (Satou et al., 2022; Stolfi et al., 2015b) for genes examined in the present study are as follows: CG.KY21.Chr12.158 for *Foxc*, CG. KY21.Chr8.693 for *Foxg*, CG.KY21.Chr2.381 for *Admp*, CG.KY21.Chr4.346 for *Bmp2/4*, CG.KY21.Chr2.933 for *Bmp5/6/7/8*, CG.KY21.Chr12.737 for *Noggin*, CG.KY21.Chr6.382 for *Chordin*, CG.KY21.Chr3.541 for *Six1/2*, and CG.KY21.Chr13.415 for *Zf220*.

Functional assays

Dorsomorphin, an inhibitor of BMP signaling (Wako, #044-33751), was applied to embryos at a concentration of 50 μM. The upstream sequence of *Foxc* [nucleotide positions 1,011,273 to 1,013,312 on chromosome 12 of the HT version of the assembly (Satou et al., 2019)], which directs expression in ANB cells (Liu and Satou, 2019; Wagner and Levine, 2012), was used for misexpression of *Noggin* and *Chordin*. To mark ANB cells, the same upstream sequence was used to direct *GFP* expression. These constructs were introduced into fertilized eggs by electroporation. An antisense morpholino oligonucleotide against *Admp*, which was used previously (Imai et al., 2012; Imai et al., 2006; Waki et al., 2015) (5'-TATCGTGTAGTTTGCTTTCTATATA-3'), was introduced into eggs by microinjection. All functional assays were performed at least twice using different batches of embryos.

In situ hybridization and immunostaining

For whole-mount *in situ* hybridization, digoxigenin (DIG)-RNA probes were synthesized by *in vitro* transcription with T7 RNA polymerase. Embryos were fixed in 4% paraformaldehyde in 0.1 M MOPS-NaOH (pH 7.5) and 0.5 M NaCl at 4°C overnight and then stored in 80% ethanol. After washing with a phosphate-buffered saline wash containing 0.1% tween 20 (PBST), embryos were treated with 2 μg/mL Proteinase K for 30 min at 37°C, washed again with PBST, and fixed with 4% paraformaldehyde for 1 h at room temperature.

110 Embryos were then incubated in 6x saline sodium citrate buffer (SSC), 50% formamide, 5x
111 Denhardt's solution, 100 μg/mL yeast tRNA, and 0.1% tween 20 for 1 h at 50°C. After this
112 pre-hybridization step, specific RNA probes were added and incubated for 48 h at 50°C.
113 Embryos were treated with RNase A, and incubated in 0.5x SSC, 50% formamide, and 0.1%
114 tween 20 for 15 min at 50°C twice. Embryos were further incubated in 0.5% blocking reagent
115 (Roche) in PBST for 30 min, and then in 1:2000 alkaline-phosphatase-conjugated anti-DIG
116 antibody (Roche). For chromogenic detection, embryos were further washed with 0.1 M
117 NaCl, 50 mM $MgCl_2$, and 0.1 M Tris-HCl (pH 9.5). Then NBT and BCIP were used for
118 detection. For fluorescent detection, we used the TSA plus system (Perkin Elmer,
119 #NEL753001KT).

120 For immunostaining, embryos were fixed with 3.7% formaldehyde, and treated with 3%
121 H_2O_2 for 30 min to quench endogenous peroxidase activity. Then they were incubated
122 overnight with an anti-phosphoryrated-Smad1 antibody (1:1000, Abcam, #ab97689) in Can-
123 Get-Signal-Immunostain Solution B (TOYOBO, #NKB-601). The signal was visualized with
124 a TSA Kit (Invitrogen, #T30953) using HRP-conjugated goat anti-rabbit IgG and Alexa Fluor
125 555 tyramide. GFP protein was similarly detected with an antibody against GFP (1:300, MBL,
126 #M048-3). Fluorescence intensities were quantified with ImageJ software (Schneider et al.,
127 2012), and represented as relative intensities, which were calculated by dividing sums of
128 pSmad1/5/9 signals of four ANB cells with sums of DAPI signals of the same cells.

Results

BMP signaling is activated in ANB cells

To understand exactly how BMP signaling influences patterning of ANB cells, we first examined whether BMP signaling is activated in ANB cells by an antibody against phosphorylated Smad1, which was previously used to detect phosphorylated Smad1/5/9 (pSmad1/5/9) in ascidian embryos (Waki, Imai, & Satou, 2015). To mark ANB cells, we introduced a reporter construct containing a fusion gene of *GFP* and the *Foxc* upstream regulator sequence (*Foxc>GFP*). At the gastrula stage, immunostaining signals for pSamd1/5/9 were detected in all ANB cells marked with GFP, although the medial two cells in the anterior row (a9.40 cells) showed much stronger signals than the other ANB cells (Figure 1B). At the early neurula stage, these cells divide along the anterior-posterior axis to make four rows. The central cells of the anterior two rows (a10.79 and a10.80, which are daughter cells of a9.40) showed stronger signals than the remaining ANB cells (Figure 1C).

Admp is expressed in ANB cells

Next, we tried to identify a BMP ligand responsible for activation of BMP signaling in the ANB region. In the ascidian genome, four BMP ligand genes are encoded (Hino et al., 2003). Among them, *Bmp3* is not expressed at the gastrula or neurula stages (Imai et al., 2004), and *Bmp2/4* is activated under control of *Admp* (Imai et al., 2012; Waki et al., 2015). Therefore, we determined precise identities of cells that expressed the remaining two ligand genes, *Admp* and *Bmp5/6/7/8*, by *in situ* hybridization. *Admp* was expressed in all ANB cells that express *Foxc* at the late gastrula stage (Figure 2AB). Expression of *Admp* was also observed in all ANB cells of early neurula embryos, in which the most anterior and posterior rows of ANB cells are marked by *Foxg* expression (Figure 2CD). On the other hand, *Bmp5/6/7/8* began to be expressed weakly in the most anterior row of ANB cells at the early neurula stage (Figure 2EF). This gene was also expressed in an anterior row of neural plate. There was one row of cells between the posterior row of ANB cells and the row of the neural plate cells with *Bmp5/6/7/8* expression. Expression of *Bmp5/6/7/8* in the anterior ANB cells was transient, and disappeared by the middle neurula stage (Figure 2G).

157 Because *Admp*, but not *Bmp5/6/7/8*, was expressed in ANB cells of late gastrula
158 embryos, we reasoned that *Admp* is mainly responsible for activation of BMP signaling in the
159 ANB region. To confirm this hypothesis, we injected an antisense morpholino oligonucleotide
160 against *Admp*. Signal intensity of immunostaining for pSmad1/5/9 was greatly reduced in
161 *Admp* morphant embryos, indicating a primary role of *Admp* in activating BMP signaling in
162 this region (Figure 2H–J). Because *Admp* is expressed in early embryos (Imai et al., 2004;
163 Imai et al., 2006; Oda-Ishii et al., 2016; Pasini et al., 2006; Tokuoka et al., 2021), we cannot
164 completely rule out the possibility that *Admp* expressed in early embryos indirectly regulates
165 BMP signaling in the ANB cells. It is also possible that *Admp* expressed in cells other than
166 ANB cells activate BMP signaling in the ANB region, because Admp is a secreted molecule.
167 However, the knockdown result and the observation that *Admp* was expressed in all ANB
168 cells agreed with the above hypothesis that *Admp* is mainly responsible for activation of BMP
169 signaling in the ANB region.

170 ***Chordin* and *Noggin* are expressed in cells lateral and posterior to the adjacent ANB**
171 **region**

172 The expression pattern of *Admp* was not perfectly consistent with the pattern of
173 pSmad1/5/9 signals (compare Figure 1 to Figure 2). Therefore, we examined expression
174 patterns of genes encoding secreted BMP-antagonists, which can act non-cell-autonomously.
175 At the late gastrula stage, *Chordin* was expressed on both sides of the neural plate, as
176 previously reported (Abitua et al., 2015; Hudson and Yasuo, 2005). At this stage, the most
177 anterior cells with *Chordin* expression were adjacent to the lateral ANB cells (Figure 3A).
178 *Noggin* was expressed in the neurula plate and the expression domain was adjacent to the
179 posterior row of ANB cells (Figure 3B). At the early neurula stage, the lateral and posterior
180 boundaries of the ANB region are still flanked with cells expressing *Chordin* and *Noggin*,
181 respectively (Figure 3C D). Thus, expression patterns of *Chordin* and *Noggin* in the ANB
182 region account for the immunostaining pattern for pSmad1/5/9. Indeed, overexpression of
183 *Chordin* and *Noggin* in the ANB region using the *Foxc* regulatory region weakened the level
184 of pSmad1/5/9 staining (Figure 3EF). Note that the pSmad1/5/9 staining was also weakened
185 in cells that do not express *Foxc* because *Chordin* and *Noggin* are secreted antagonists.

186 **Expression of *Foxg* and *Six1/2* in the ANB region requires BMP signaling**

187 To examine whether BMP signaling is necessary for gene expression in the ANB region,
188 we misexpressed *Noggin* in ANB cells using the upstream regulatory sequence of *Foxc*
189 (*Foxc>Noggin*). *Foxg* expression was clearly downregulated in the posterior row of 82% of
190 these experimental embryos, and also in the anterior row of 7% of embryos (Figure 4AB).
191 Next, embryos introduced with the *Foxc>Noggin* construct were treated with dorsomorphin,
192 which is an inhibitor of BMP signaling and has been used in this animal (Ohta and Satou,
193 2013; Waki et al., 2015), from the early gastrula stage. Because DNA constructs introduced
194 by electroporation may not be expressed in all ANB cells, we expected BMP signaling levels
195 to be further reduced by dorsomorphin treatment. All of these embryos lost *Foxg* expression
196 in the posterior row, and 31% of these embryos additionally lost *Foxg* expression in the
197 anterior row (Figure 4B). These results indicate that BMP signaling is required for *Foxg*
198 expression in the ANB region, although *Foxg* expression is more sensitive to dorsomorphin in
199 the posterior row than in the anterior row.

200 Next, we examined *Six1/2* expression in the above two types of experimental embryo. In
201 93% of embryos electroporated with *Foxc>Noggin*, *Six1/2* expression was reduced (Figure
202 4CD). Notably, 18% of embryos lost *Six1/2* expression completely in the ANB region,
203 indicating that BMP signaling is required for *Six1/2* expression in the ANB region. On the
204 other hand, in the experiment in which we additionally treated embryos with dorsomorphin,
205 *Six1/2* expression was lost in only 63%. We did not find any embryos that completely lost
206 *Six1/2* expression in the ANB region, raising the possibility that *Six1/2* is also expressed in
207 cells with a very low level or absence of BMP signaling.

208 To confirm this hypothesis, we injected various concentrations of *Foxc>Noggin* into
209 eggs. While less than 10% of these embryos lost *Six1/2* expression in the most posterior cells
210 at low concentrations (1 or 5 ng/μL), 24 to 31% of embryos lost *Six1/2* expression at high
211 concentrations (10, 15, or 20 ng/μL) (Figure 4E). The percentage of embryos that lost *Six1/2*
212 expression is slightly lower at 20 ng/μL than at 10 or 15 ng/μL. These observations are
213 consistent with the hypothesis that BMP signaling is necessary for *Six1/2* expression in the

214 posterior row, but a very low level or absence of BMP signaling can also induce *Six1/2*
215 expression.

216 Next, we counted embryos with ectopic expression in the same specimens. While ectopic
217 expression was hardly observed at low concentrations, it was observed in almost all embryos
218 at 15 and 20 ng/μL (Figure 4FG). This observation is consistent with the hypothesis that a
219 very low level or lack of BMP signaling can induce *Six1/2* expression.

220 **BMP signaling activity is required for proper palp formation**

221 Larval palps are derived from the anterior three rows of ANB cells at the neurula stage.
222 The most anterior row gives rise to protrusive structures and the middle two rows give rise to
223 basal cells surrounding the protrusions (Cao et al., 2019; Ikeda et al., 2013; Liu & Satou,
224 2019; Wagner & Levine, 2012; Wagner et al., 2014). Normal larvae have three protrusions
225 (two are seen in Figure 5A). Larvae with the misexpression construct of *Noggin* developed
226 one large protrusion (Figure 5B), suggesting that BMP signaling is involved in palp
227 formation.

228 We previously reported that larvae in which *Foxg* is misexpressed in all ANB cells also
229 develop one large palp (Liu and Satou, 2019). Therefore, we examined whether
230 misexpression of *Noggin* induced ectopic *Foxg* expression. In normal development, *Foxg*
231 expression becomes rarely visible at the early tailbud stage, but soon after it is reactivated in
232 three clusters of cells, which are descendants of the most anterior row cells (Figure 5C), each
233 of which gives rise to a palp protrusion, as previously shown (Liu and Satou, 2019). On the
234 other hand, in embryos with the *Noggin* misexpression construct, *Foxg* was expressed
235 ectopically in gaps between these clusters, and the *Foxg* expression domain became a single
236 arc (Figure 5D). Similarly, in tailbud embryos treated with dorsomorphin from the middle
237 neurula stage, at the time when *Foxg* begins to be expressed in the ANB region, *Foxg* was
238 expressed ectopically in a single arc, while it was normally expressed in control embryos
239 treated with DMSO (Figure 5E, F).

240 At the tailbud stage, *Zf220* represses *Foxg* in cells between the clusters where *Foxg* is
241 normally expressed (Liu and Satou, 2019). We therefore hypothesized that *Zf220* might be

242 downregulated in embryos in which BMP signaling was inhibited. In normal embryos, *Zf220*
243 was expressed in cells between the clusters of cells with *Foxg* expression (Figure 5G), as
244 previously shown (Liu & Satou, 2019). On the other hand, expression of *Zf220* in the
245 intervening cells was downregulated in almost all (94%) embryos treated with dorsomorphin
246 from the gastrula stage (Figure 5H). Thus, BMP activity is required for *Zf220* expression in
247 these intervening cells. *Zf220* is also expressed in the both ends of the anterior rows, and this
248 expression was also affected in 52% of the embryos (Figure 5I). Intervening cells that lost
249 *Zf220* are derived from a10.80 in the most anterior row and a10.79 in the second row, and
250 these parental cells showed strong pSmad1/5/9 signals at the early neurula stage (Figure
251 1DE). On the other hand, flanking cells, in which *Zf220* expression was less affected, are
252 derived from a10.72 in the most anterior row and a10.71 in the second row, and these parental
253 cells showed weak pSmad1/5/9 signals at the early neurula stage (Figure 1DE). Thus,
254 expression of *Zf220* in medial cells is under control of BMP signaling, and also weakly
255 regulated by BMP signaling in the flanking cells.

256 **Discussion**

257 At the late gastrula and early neurula stages, BMP signaling is activated in ANB cells.
258 Our data indicate that Admp activates BMP signaling in the ANB region, and that Chordin
259 and Noggin restrict the region with BMP signaling activity to the ANB region and prevent it
260 from expanding to the neural plate. Because *Bmp2/4* is activated under control of *Admp* (Imai
261 et al., 2012; Waki et al., 2015), it is possible that Bmp2/4 also acts in this region. Although
262 these factors create a graded pattern of BMP signaling, the difference in intensity of BMP
263 signaling within the ANB region is not important for *Foxg* and *Six1/2* expression at the late
264 gastrula stage, because a low level of BMP signaling is sufficient for expression of these
265 genes. In addition, since *Foxg* expression is restricted to the most anterior and posterior rows
266 of the ANB region by the action of the MAPK signaling, BMP signaling may not be required
267 for positional information, and may have a permissive role.

268 Our results showed that *Six1/2* expression in the ANB region normally requires BMP
269 signaling, because reduction of BMP signaling levels by misexpression of *Noggin* resulted in
270 loss of *Six1/2* expression. However, because *Six1/2* expression was seen in embryos in which
271 BMP signaling levels were further reduced by additional treatment with dorsomorphin, it is
272 likely that *Six1/2* expression is also induced at a very low level or even an absence of BMP
273 signaling. This is consistent with expression of *Six1/2* in cells flanking the ANB region. In
274 these flanking cells, *Chordin* is expressed and pSmad1/5/8 was scarcely detected. In addition,
275 because a previous study showed that overexpression of *Bmp2/4* suppressed *Six1/2* expression
276 (Abitua et al., 2015), it is likely that *Six1/2* expression is induced at modest, or very low (or
277 negligible) levels of BMP signaling, and is suppressed at a high level or between the modest
278 and very low levels.

279 At the late neurula stage, *Zf220* begins to be expressed in descendants of cells that show
280 strong signals for pSmad1/5/9, and *Zf220* expression in these descendants is under control of
281 BMP signaling. Although it remains to be clarified how *Zf220* is expressed in only some of
282 these descendant cells, it is possible that BMP signaling has an instructive role in activating
283 *Zf220* in these cells. *Zf220* is also expressed in descendants of cells that showed weak signals
284 for pSmad1/5/9. However, in these cells, *Zf220* expression was less sensitive to

downregulation of BMP signaling; therefore, regulation of *Zf220* in these cells differs from that in medial cells.

Thus, BMP signaling positively regulates gene expression in the ANB region, which is thought to share an evolutionary origin with vertebrate cranial placodes (Abitua et al., 2015; Graham and Shimeld, 2013; Ikeda et al., 2013; Ikeda and Satou, 2017; Liu and Satou, 2019; Manni et al., 2005; Manni et al., 2004; Mazet et al., 2005; Wagner and Levine, 2012). In vertebrate embryos, it has been proposed that ectodermal cells are induced by BMP, giving rise to epidermis, pre-placodal ectoderm, neural crest, and neural plate at different BMP concentrations, although specification of pre-placodal ectoderm and neural crest have different requirements for additional signaling molecules and for BMP signaling at different times (Ahrens and Schlosser, 2005; Brugmann and Moody, 2005; Glavic et al., 2004; Kwon et al., 2010; Steventon et al., 2014; Tribulo et al., 2003). Thus, ANB cells of ascidians and pre-placodal cells of vertebrates commonly use BMP signals for specification.

In ascidian embryos, there are cell populations that arguably share their evolutionary origins with vertebrate neural crest cells (Abitua et al., 2012; Stolfi et al., 2015a; Waki et al., 2015). It has not been determined whether BMP signaling is involved in specification of these neural-crest-like cells in ascidian embryos. However, in ascidian embryos, cell lineages of these neural-crest-like cells are clearly distinct from the cell lineage of the ANB. This means that there is no cell population that has potential to become both ANB cells and neural-crest-like cells in ascidian embryos; therefore, it is unlikely that a gradient of BMP signaling is required in this animal to specify a cell population that has bipotential to give rise to these two cell populations. Nevertheless, the requirement of BMP signaling for gene expression in the ANB region of ascidian embryos further supports the hypothesis that ANB cells share an evolutionary origin with vertebrate cranial placodes.

Acknowledgements

We thank Reiji Masuda, Shinichi Tokuhiro, Chikako Imaizumi (Kyoto University), Manabu Yoshida (University of Tokyo), and other members working under the National BioResource Project for *Ciona* (MEXT, Japan) at Kyoto University. We also thank the University of Tokyo for providing experimental animals.

Author contribution

BL and XR performed experiments. BL and YS drafted the original manuscript. BL, XR, and YS reviewed the manuscript draft, revised it, and approved the final version.

Funding

This research was supported by grants from the Japan Society for the Promotion of Science under the grant numbers 21H02486 and 21H05239 to YS**.**

Data availability

All data generated or analyzed during this study are included in this published article.

Competing interests

The authors declare no competing interests.

References

Abitua, P.B., Gainous, T.B., Kaczmarczyk, A.N., Winchell, C.J., Hudson, C., Kamata, K., Nakagawa, M., Tsuda, M., Kusakabe, T.G., Levine, M., (2015) The pre-vertebrate origins of neurogenic placodes. Nature 524: 462-465. https://doi.org/10.1038/nature14657

Abitua, P.B., Wagner, E., Navarrete, I.A., Levine, M., (2012) Identification of a rudimentary neural crest in a non-vertebrate chordate. Nature 492: 104-107. https://doi.org/10.1038/nature11589

Ahrens, K., Schlosser, G., (2005) Tissues and signals involved in the induction of placodal Six1 expression in Xenopus laevis. Developmental Biology 288: 40-59. https://doi.org/10.1016/j.ydbio.2005.07.022

Brugmann, S.A., Moody, S.A., (2005) Induction and specification of the vertebrate ectodermal placodes: precursors of the cranial sensory organs. Biology of the cell / under the auspices of the European Cell Biology Organization 97: 303-319. https://doi.org/10.1042/BC20040515

Brugmann, S.A., Pandur, P.D., Kenyon, K.L., Pignoni, F., Moody, S.A., (2004) Six1 promotes a placodal fate within the lateral neurogenic ectoderm by functioning as both a transcriptional activator and repressor. Development 131: 5871-5881. https://doi.org/10.1242/dev.01516

Cao, C., Lemaire, L.A., Wang, W., Yoon, P.H., Choi, Y.A., Parsons, L.R., Matese, J.C., Wang, W., Levine, M., Chen, K., (2019) Comprehensive single-cell transcriptome lineages of a proto-vertebrate. Nature 571: 349-354. https://doi.org/10.1038/s41586-019-1385-y

Delsuc, F., Brinkmann, H., Chourrout, D., Philippe, H., (2006) Tunicates and not cephalochordates are the closest living relatives of vertebrates. Nature 439: 965-968. https://doi.org/10.1038/nature04336

Esterberg, R., Fritz, A., (2009) dlx3b/4b are required for the formation of the preplacodal region and otic placode through local modulation of BMP activity. Developmental Biology 325: 189-199. https://doi.org/10.1016/j.ydbio.2008.10.017

Gans, C., Northcutt, R.G., (1983) Neural Crest and the Origin of Vertebrates - a New Head. Science 220: 268-273. https://doi.org/DOI 10.1126/science.220.4594.268

Glavic, A., Honore, S.M., Feijoo, C.G., Bastidas, F., Allende, M.L., Mayor, R., (2004) Role of BMP signaling and the homeoprotein iroquois in the specification of the cranial placodal field. Developmental Biology 272: 89-103. https://doi.org/10.1016/j.ydbio.2004.04.020

Graham, A., Shimeld, S.M., (2013) The origin and evolution of the ectodermal placodes. Journal of anatomy 222: 32-40. https://doi.org/10.1111/j.1469-7580.2012.01506.x

Hino, K., Satou, Y., Yagi, K., Satoh, N., (2003) A genomewide survey of developmentally relevant genes in Ciona intestinalis. VI. Genes for Wnt, TGFbeta, Hedgehog and JAK/STAT signaling pathways. Dev Genes Evol 213: 264-272. https://doi.org/10.1007/s00427-003-0318-8

Horie, R., Hazbun, A., Chen, K., Cao, C., Levine, M., Horie, T., (2018) Shared evolutionary origin of vertebrate neural crest and cranial placodes. Nature 560: 228-232. https://doi.org/10.1038/s41586-018-0385-7

Hudson, C., Yasuo, H., (2005) Patterning across the ascidian neural plate by lateral Nodal signalling sources. Development 132: 1199-1210. https://doi.org/10.1242/dev.01688

Ikeda, T., Matsuoka, T., Satou, Y., (2013) A time delay gene circuit is required for palp formation in the ascidian embryo. Development 140: 4703-4708. https://doi.org/10.1242/dev.100339

Ikeda, T., Satou, Y., (2017) Differential temporal control of *Foxa.a* and *Zic-r.b* specifies brain versus notochord fate in the ascidian embryo. Development 144: 38-43. https://doi.org/10.1242/dev.142174

Imai, K.S., Daido, Y., Kusakabe, T.G., Satou, Y., (2012) Cis-acting transcriptional repression establishes a sharp boundary in chordate embryos. Science 337: 964-967. https://doi.org/10.1126/science.1222488

Imai, K.S., Hino, K., Yagi, K., Satoh, N., Satou, Y., (2004) Gene expression profiles of transcription factors and signaling molecules in the ascidian embryo: towards a comprehensive understanding of gene networks. Development 131: 4047-4058. https://doi.org/10.1242/dev.01270

Imai, K.S., Levine, M., Satoh, N., Satou, Y., (2006) Regulatory blueprint for a chordate embryo. Science 312: 1183-1187. https://doi.org/10.1126/science.1123404

Kwon, H.J., Bhat, N., Sweet, E.M., Cornell, R.A., Riley, B.B., (2010) Identification of Early Requirements for Preplacodal Ectoderm and Sensory Organ Development. PLoS genetics 6. https://doi.org/ARTN e1001133

10.1371/journal.pgen.1001133

Litsiou, A., Hanson, S., Streit, A., (2005) A balance of FGF, BMP and WNT signalling positions the future placode territory in the head. Development 132: 4051-4062. https://doi.org/10.1242/dev.01964

Liu, B., Satou, Y., (2019) Foxg specifies sensory neurons in the anterior neural plate border of the ascidian embryo. Nat Commun 10: 4911. https://doi.org/10.1038/s41467-019-12839-6

Liu, B., Satou, Y., (2020) The genetic program to specify ectodermal cells in ascidian embryos. Dev Growth Differ 62: 301-310. https://doi.org/10.1111/dgd.12660

Manni, L., Agnoletto, A., Zaniolo, G., Burighel, P., (2005) Stomodeal and neurohypophysial placodes in Ciona intestinalis: insights into the origin of the pituitary gland. Journal of experimental zoology. Part B, Molecular and developmental evolution 304: 324-339. https://doi.org/10.1002/jez.b.21039

Manni, L., Lane, N.J., Joly, J.S., Gasparini, F., Tiozzo, S., Caicci, F., Zaniolo, G., Burighel, P., (2004) Neurogenic and non-neurogenic placodes in ascidians. Journal of experimental zoology. Part B, Molecular and developmental evolution 302: 483-504. https://doi.org/10.1002/jez.b.21013

Mazet, F., Hutt, J.A., Milloz, J., Millard, J., Graham, A., Shimeld, S.M., (2005) Molecular evidence from Ciona intestinalis for the evolutionary origin of vertebrate sensory placodes. Dev Biol 282: 494-508. https://doi.org/10.1016/j.ydbio.2005.02.021

Oda-Ishii, I., Kubo, A., Kari, W., Suzuki, N., Rothbacher, U., Satou, Y., (2016) A maternal system initiating the zygotic developmental program through combinatorial repression in the ascidian embryo. PLoS genetics 12: e1006045. https://doi.org/10.1371/journal.pgen.1006045

Ohta, N., Satou, Y., (2013) Multiple signaling pathways coordinate to induce a threshold response in a chordate embryo. PLoS genetics 9: e1003818. https://doi.org/10.1371/journal.pgen.1003818

Pasini, A., Amiel, A., Rothbacher, U., Roure, A., Lemaire, P., Darras, S., (2006) Formation of the ascidian epidermal sensory neurons: insights into the origin of the chordate peripheral nervous system. PLoS Biol 4: e225. https://doi.org/10.1371/journal.pbio.0040225

Putnam, N.H., Butts, T., Ferrier, D.E., Furlong, R.F., Hellsten, U., Kawashima, T., Robinson-Rechavi, M., Shoguchi, E., Terry, A., Yu, J.K., Benito-Gutierrez, E.L., Dubchak, I., Garcia-Fernandez, J., Gibson-Brown, J.J., Grigoriev, I.V., Horton, A.C., de Jong, P.J., Jurka, J., Kapitonov, V.V., Kohara, Y., Kuroki, Y., Lindquist, E., Lucas, S., Osoegawa, K., Pennacchio, L.A., Salamov, A.A., Satou, Y., Sauka-Spengler, T., Schmutz, J., Shin, I.T., Toyoda, A., Bronner-Fraser, M., Fujiyama, A., Holland, L.Z., Holland, P.W., Satoh, N., Rokhsar, D.S., (2008) The amphioxus genome and the evolution of the chordate karyotype. Nature 453: 1064-1071. https://doi.org/10.1038/nature06967

Satou, Y., Kawashima, T., Shoguchi, E., Nakayama, A., Satoh, N., (2005) An integrated database of the

ascidian, *Ciona intestinalis*: Towards functional genomics. Zool Sci 22: 837-843. https://doi.org/10.2108/zsj.22.837

Satou, Y., Nakamura, R., Yu, D., Yoshida, R., Hamada, M., Fujie, M., Hisata, K., Takeda, H., Satoh, N., (2019) A nearly complete genome of *Ciona intestinalis* type A (*C. robusta*) reveals the contribution of inversion to chromosomal evolution in the genus *Ciona*. Genome biology and evolution 11: 3144-3157. https://doi.org/10.1093/gbe/evz228

Satou, Y., Tokuoka, M., Oda-Ishii, I., Tokuhiro, S., Ishida, T., Liu, B., Iwamura, Y., (2022) A Manually Curated Gene Model Set for an Ascidian, *Ciona robusta* (*Ciona intestinalis* Type A). Zool Sci 39: 253-260. https://doi.org/10.2108/zs210102

Schlosser, G., (2014) Early embryonic specification of vertebrate cranial placodes. Wires Dev Biol 3: 349-363. https://doi.org/10.1002/wdev.142

Schneider, C.A., Rasband, W.S., Eliceiri, K.W., (2012) NIH Image to ImageJ: 25 years of image analysis. Nature methods 9: 671-675. https://doi.org/10.1038/nmeth.2089

Singh, S., Groves, A.K., (2016) The molecular basis of craniofacial placode development. Wiley Interdiscip Rev Dev Biol 5: 363-376. https://doi.org/10.1002/wdev.226

Steventon, B., Mayor, R., Streit, A., (2014) Neural crest and placode interaction during the development of the cranial sensory system. Dev Biol 389: 28-38. https://doi.org/10.1016/j.ydbio.2014.01.021

Stolfi, A., Ryan, K., Meinertzhagen, I.A., Christiaen, L., (2015a) Migratory neuronal progenitors arise from the neural plate borders in tunicates. Nature 527: 371-374. https://doi.org/10.1038/nature15758

Stolfi, A., Sasakura, Y., Chalopin, D., Satou, Y., Christiaen, L., Dantec, C., Endo, T., Naville, M., Nishida, H., Swalla, B.J., Volff, J.N., Voskoboynik, A., Dauga, D., Lemaire, P., (2015b) Guidelines for the nomenclature of genetic elements in tunicate genomes. Genesis 53: 1-14. https://doi.org/10.1002/dvg.22822

Tokuoka, M., Maeda, K., Kobayashi, K., Mochizuki, A., Satou, Y., (2021) The gene regulatory system for specifying germ layers in early embryos of the simple chordate. Sci Adv 7: eabf8210. https://doi.org/10.1126/sciadv.abf8210

Tribulo, C., Aybar, M.J., Nguyen, V.H., Mullins, M.C., Mayor, R., (2003) Regulation of Msx genes by a Bmp gradient is essential for neural crest specification. Development 130: 6441-6452. https://doi.org/10.1242/dev.00878

Wagner, E., Levine, M., (2012) FGF signaling establishes the anterior border of the Ciona neural tube. Development 139: 2351-2359. https://doi.org/10.1242/dev.078485

Wagner, E., Stolfi, A., Choi, Y.G., Levine, M., (2014) Islet is a key determinant of ascidian palp morphogenesis. Development 141: 3084-3092. https://doi.org/10.1242/dev.110684

Waki, K., Imai, K.S., Satou, Y., (2015) Genetic pathways for differentiation of the peripheral nervous system in ascidians. Nat Commun 6: 8719. https://doi.org/10.1038/ncomms9719

Liu et al., Figure 1

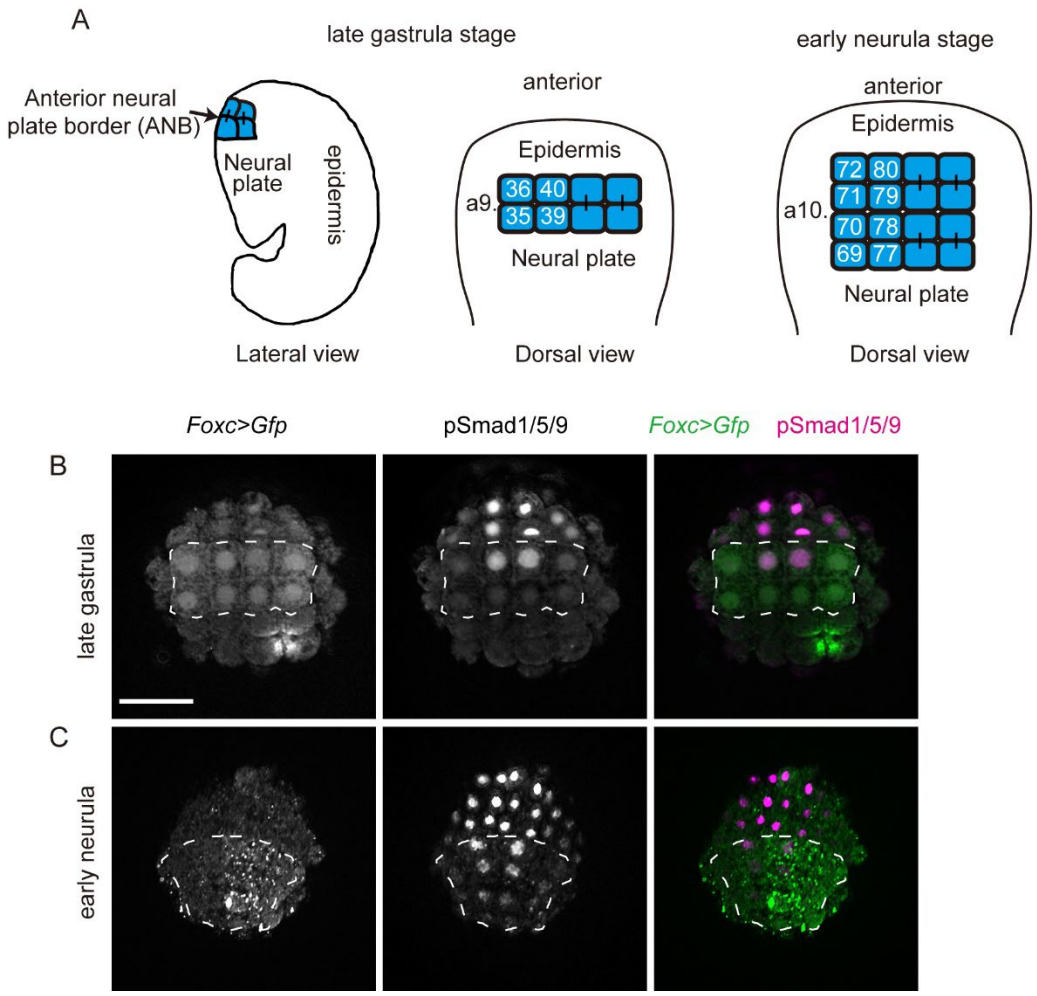

Figure 1. BMP signaling is activated in ANB cells. (A) Schematic illustration of the anterior border of the neural plate in ascidian late gastrula and early neurula embryos. Because embryos are bilaterally symmetrical, names of individual cells are indicated only in the left half, and are prefixed with IDs shown next to the illustration, e.g., the left upper cell of the late gastrula embryo is called a9.36. Vertical bars indicate sister cell relationships. (B, C) Immunostaining of (B) a late gastrula embryo and (C) an early neurula embryo to detect phosphorylated Smad1/5/9 (pSmad1/5/9). ANB cells were marked by *Foxc>GFP* expression, detected with an anti-GFP antibody. Note that GFP was detected only on the right side because of mosaic incorporation. Right images are overlaid in pseudocolor. The brightness and contrast of these photographs were adjusted linearly. ANB cells are enclosed by broken lines. Note that strong signals are observed in the anterior medial ANB cells and relatively weak signals are also observed in the remaining ANB cells. Dorsal views are shown. The scale bar in (B) represents 50 μm.

Liu et al., Figure 2

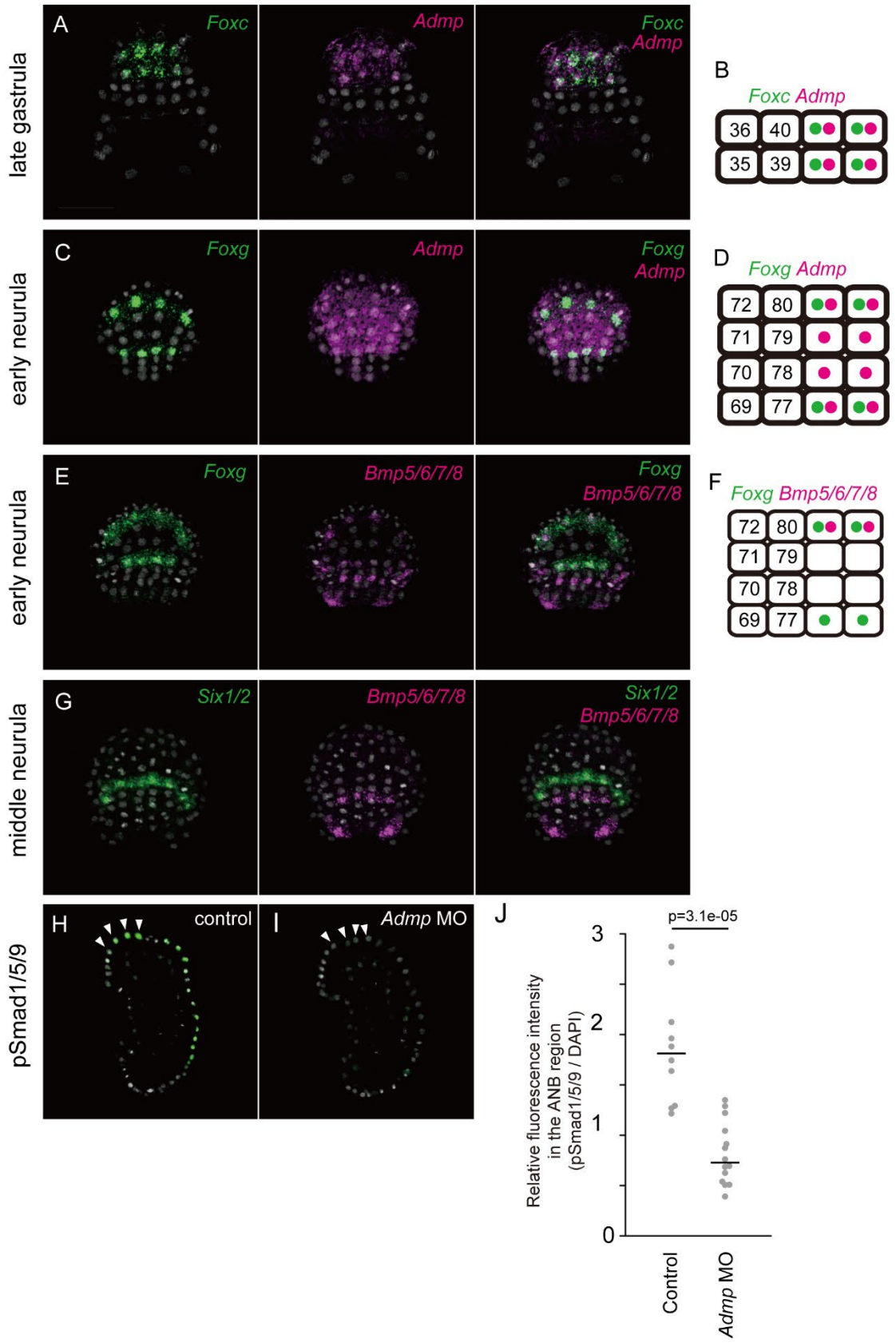

467

Figure 2. *Admp* and *BMP5/6/7/8* are expressed in ANB cells. (A-G) *In situ* hybridization for (A,C) *Admp* (magenta) expression at (A) the late gastrula stage and (C) early neurula stage, and for (E, G) *Bmp5/6/7/8* (magenta) expression at (E) the early neurula stage and (G) the middle neurula stage. *Foxc* in (A) marks ANB cells (green). *Foxg* in (C) and (E) marks the most anterior and posterior rows of the ANB region (green). *Six1/2* marks the most posterior row of the ANB (green), although this gene is also expressed in the two flanking cells on both sides of the ANB. The results shown in (A), (C), and (E) are illustrated in (B), (D), and (F), respectively. Dorsal views are shown. (H, I) Optical slices of pSmad1/5/9 immunostaining of (H) an unperturbed control early neurula embryo and (I) an early neurula embryo injected with the *Admp* MO (green). Nuclei are stained with DAPI (gray). ANB cells are marked by arrowheads. Photographs are pseudocolored, and lateral views are shown. (J) Quantification of fluorescence intensities of signals for pSmad1/5/9 in the ANB region of control unperturbed embryos and *Admp* morphants. Each dot represents relative signal intensities of a line of four medial ANB cells, and bars represent median values. Relative intensities were calculated by dividing sums of pSmad1/5/9 signals of four ANB cells with sums of DAPI signals of the same cells. As we used tyramide signal amplification, signal levels might not be amplified linearly. However, a Wilcoxon's rank sum test indicated that signal levels are significantly different between the control and experimental specimens. The scale bar in (A) represents 50 μm.

Liu et al., Figure 3

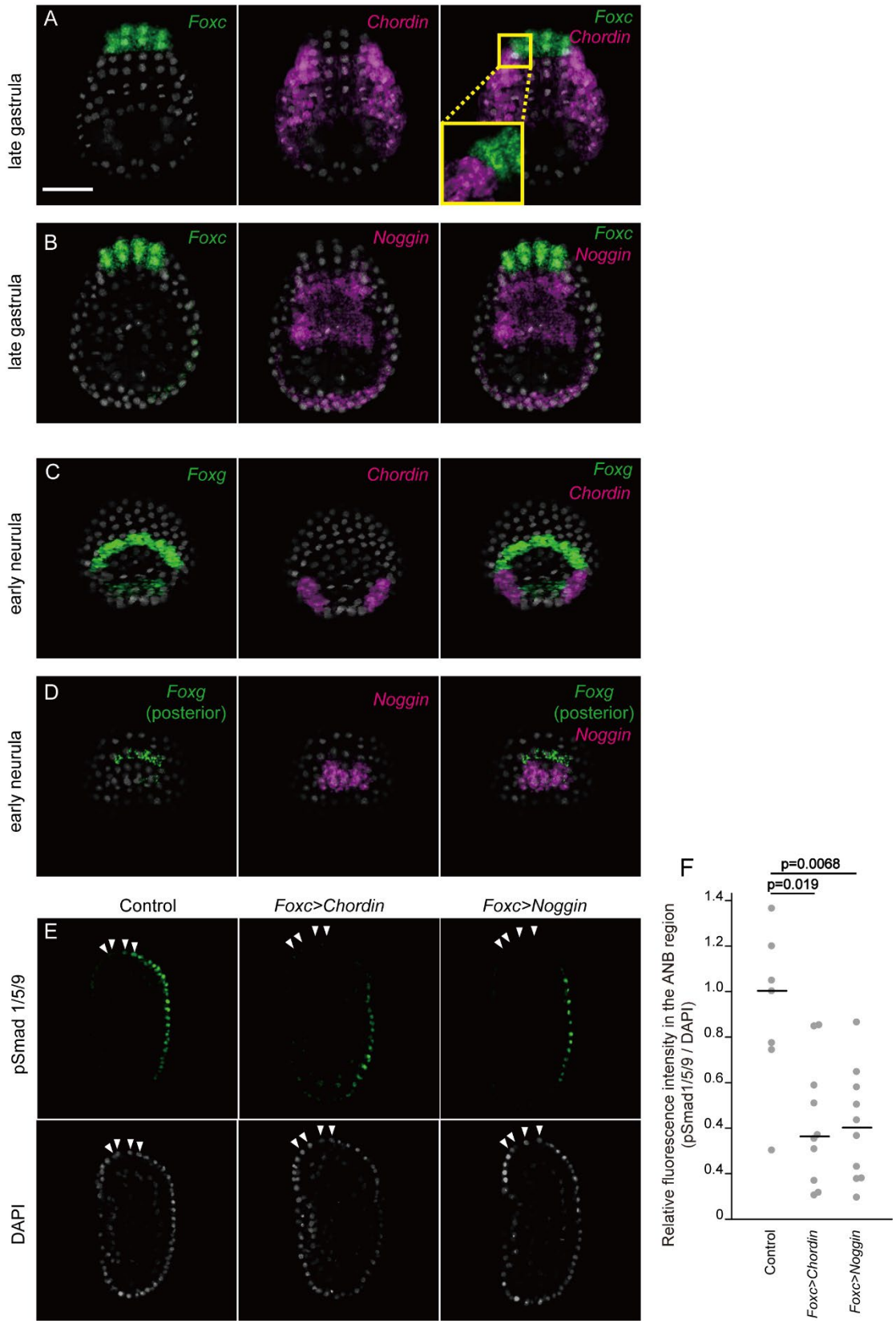

488

Figure 3. *Chordin* and *Noggin* are expressed in cells next to the ANB cells. (A-D) I*n situ* hybridization for (A) *Foxc* (green) and *Chordin* (magenta), (B) *Foxc* (green) and *Noggin* (magenta) at late gastrula stage, and for (C) *Foxg* (green) and *Chordin* (magenta), and (D) *Foxg* (green) and *Noggin* (magenta) at the early neurula stage. Nuclei were stained with DAPI (gray). Photographs are pseudocolored Z-projected image stacks. Dorsal views are shown. Note that the anterior row of the ANB is not visible in (D). (E) Optical slices of pSmad1/5/9 immunostaining of an unperturbed control early neurula embryo and early neurula embryos injected with *Foxc>Chordin* or *Foxc>Noggin*. ANB cells are marked with arrowheads. Lateral views are shown. The scale bar in (A) represents 50 μm. (F) Quantification of fluorescence intensities of signals for pSmad1/5/9 in the ANB region of unperturbed control embryos and embryos injected with *Foxc>Chordin* or *Foxc>Noggin*. Each dot represents relative signal intensities of a line of four medial ANB cells, and bars represent median values. Relative intensities were calculated by dividing sums of pSmad1/5/9 signals of four ANB cells with sums of DAPI signals of the same cells. As we used tyramide signal amplification, signal levels might not be amplified linearly. However, Wilcoxon's rank sum tests indicated that signal levels are significantly different between the control and experimental specimens.

Liu et al., Figure 4

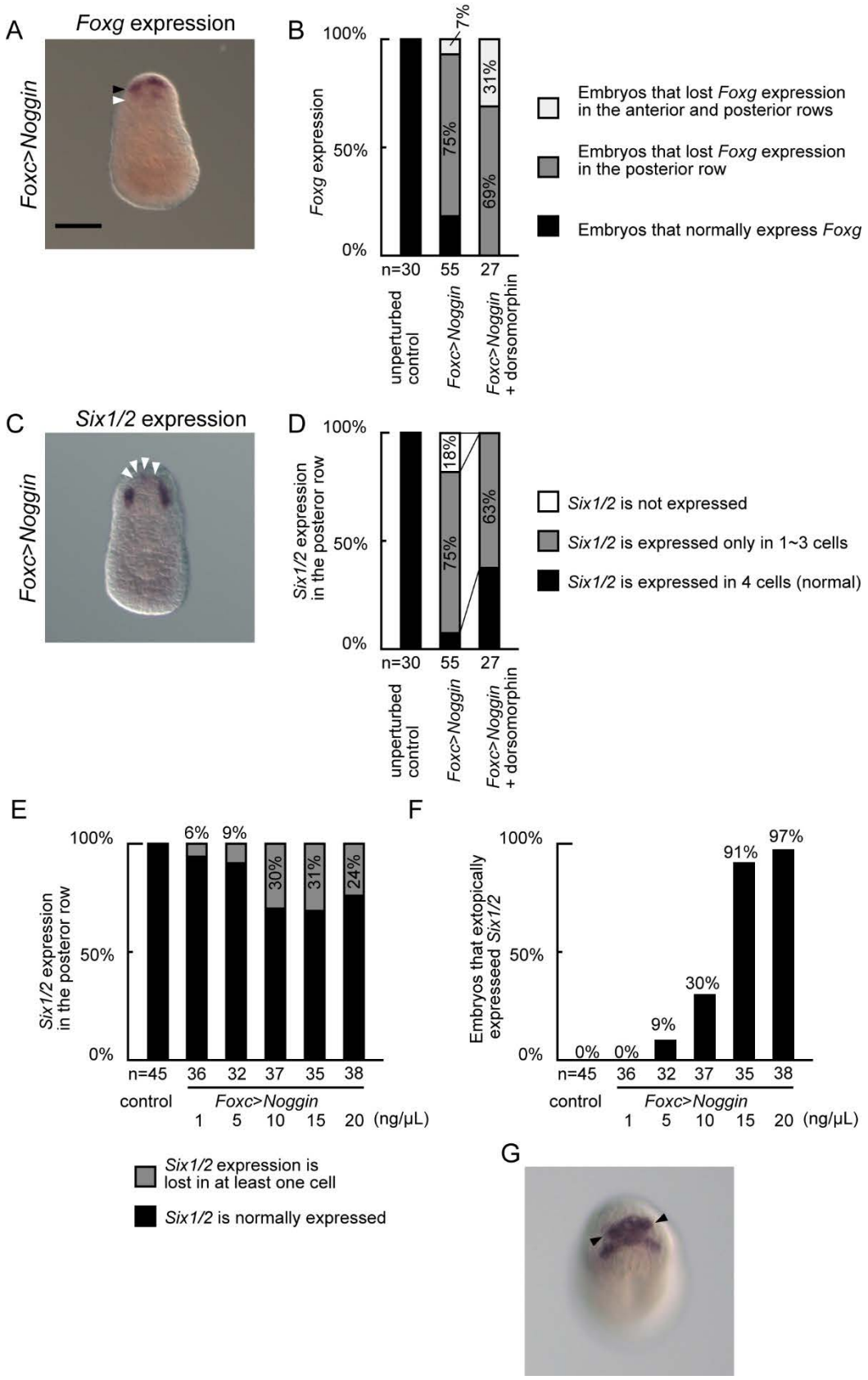

507

508 **Figure 4. Suppression of BMP signaling activity affects expression of *Foxg* and *Six1/2*.**
509 (A) A dorsal view of *in situ* hybridization for *Foxg* in an embryo in which *Foxc>Noggin* was
510 introduced by electroporation. Expression of *Foxg* in the posterior row (white arrowhead) was
511 lost, while expression in the anterior row was not affected in this embryo (black arrowhead).
512 (B) Percentages of embryos that normally expressed *Foxg*, or lost *Foxg* expression. (C) A
513 dorsal view of *in situ* hybridization for *Six1/2* in an embryo in which *Foxc>Noggin* was
514 introduced by electroporation. Expression of *Six1/2* in the ANB region was lost or greatly
515 reduced (white arrowheads). (D) Percentages of embryos that normally expressed or lost
516 *Six1/2* expression in the posterior row of the ANB region of normal and embryos
517 electroporated with *Foxc>Noggin*. (E) Percentages of embryos that normally expressed or
518 lost *Six1/2* expression in one or more ANB cells in embryos injected with *Foxc>Noggin* at
519 different concentrations. (F) Percentages of embryos that ectopically expressed *Six1/2* in
520 embryos injected with *Foxc>Noggin* at different concentrations. (G) A dorsal view of an
521 embryo in which *Foxc>Noggin* was injected at 20 ng/μL, expressed *Six1/2* ectopically
522 (arrowheads). The scale bar in (A) represents 50 μm.

523

Liu et al., Figure 5

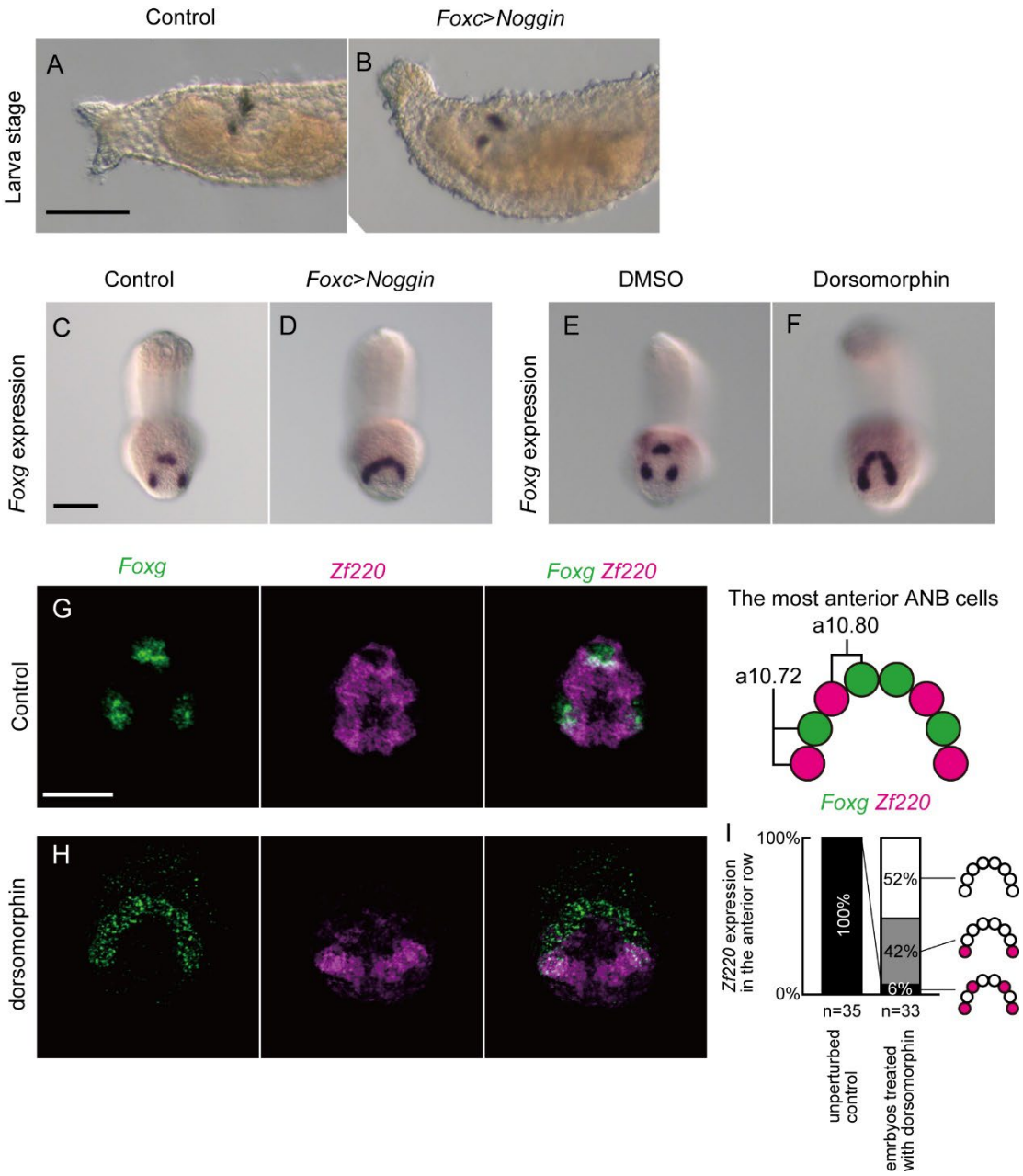

524

525 **Figure 5. BMP signaling activity is required for proper palp formation.** (A) Morphology
526 of the trunk of larvae developed from (A) a control unperturbed egg and (B) an egg
527 electroporated with the *Foxc>Noggin* construct. Two of three palp protrusions are visible in
528 this larva. We examined 16 control larvae and 24 experimental larvae, and all of them
529 exhibited phenotypes represented by these photographs. (C-F) *In situ* hybridization for *Foxg*
530 in (C) a control unperturbed embryo, (D) an embryo electroporated with the *Foxc>Noggin*
531 construct, (E) a control DMSO-treated embryo, and (F) an embryo treated with 50 μM

532 dorsomorphin at the middle tailbud stage. We examined 45 embryos electroporated with
533 *Foxc>Noggin,* and 101 embryos treated with dorsomorphin. Among them, 93% and 75% of
534 embryos exhibited the phenotypes represented in (D) and (F), respectively. (G, H) Double
535 fluorescence *in situ* hybridization for *Foxg* (green) and *Zf220* (magenta) in (G) a control
536 embryo, (H) an embryo treated with 50 μM dorsomorphin. In (H), the experimental embryo
537 lost *Zf220* in the central region, and ectopically expressed *Foxg*. The expression pattern of
538 *Foxg* and *Zf220* in the most anterior row of normal embryos are depicted on the right of (G).
539 These most-anterior-row cells are daughters of a10.72 and a10.80 as illustrated. Note that
540 *Zf220* is also expressed in the second row (Liu and Satou, 2019), which are not depicted.
541 Photographs from C to H are anterior views, and the dorsal side of the trunk is down. (I)
542 Percentages of embryos that normally expressed *Zf220* (black), lost *Zf220* expression in the
543 central cells (gray), and lost it in both of the central and flanking cells (white) in the anterior
544 row of unperturbed control embryos and embryos treated with dorsomorphin. We examined
545 *Zf220* expression by non-fluorescence *in situ* hybridization in addition to double fluorescence
546 *in situ* hybridization shown in (G) and (H). The scale bars in (A), (C), and (G) represent 50
547 μm.